Inorganica Chimica Acta 362 (2009) 3896–3900

Contents lists available at ScienceDirect

Inorganica Chimica Acta

journal homepage: www.elsevier.com/locate/ica

Preparation and characterization of mixed ammonium salts of Keggin phosphomolybdate

L. Dermeche [a], R. Thouvenot [b], S. Hocine [a], C. Rabia [a,*]

[a] Laboratoire de Chimie du Gaz Naturel, Faculté de Chimie, BP32, El-Alia, 16111 Bab-Ezzouar, Alger, Algeria
[b] Laboratoire de Chimie Inorganique et Matériaux Moléculaires, Université Pierre et Marie Curie, 4, Place Jussieu, 75252 Paris Cedex 05, France

ARTICLE INFO

Article history:
Received 2 September 2008
Received in revised form 22 April 2009
Accepted 28 April 2009
Available online 14 May 2009

Keywords:
Polyoxometalate
Keggin
Spectroscopies
Characterization

ABSTRACT

Keggin-type modified ammonium salts of molybdophosporic acid were prepared by partial substituting of the ammonium ions by X (X = Sb^{III}, Bi^{III} or Sn^{II}) ions. They were characterised by BET method, XRD, ^{31}P NMR, UV–Vis, Raman, IR spectroscopies and thermal analysis (TG and DTA). It appeared that introducing an element X = Sb or Sn led to partially reduced compound corresponding to the electron exchange occurring between Sb(III) or Sn(II) and Mo(VI) without modification of Keggin structure.

Published by Elsevier B.V.

1. Introduction

The catalytic activity of molybdophosphoric heteropolycompounds (HPA) having the Keggin structure, in oxidation reactions, depends on their reducibility. Several attempts pointed out the importance to have a reduced Keggin anion for obtaining of better selectivities towards products of partial oxidation [1]. Many studies have focused on the effect of the counter-cation nature in the polyoxometalate catalytic performances. Thus, it has been shown that the nature of cation can play a significant role in the determination of the redox processes. It has been reported that ammonium, pyridinium or quinolinium salts of phosphomolybdic acid efficiently catalyze the oxidation of propane and isobutane [2–6]. The oxidative sensitivity of these organic counter-cations allows to obtain a strong auto-reduction under thermal treatment and thus to change the redox state of the HPA without addition of reagents. Moreover, it has been shown that using Fe(III), vanadyl (VO^{2+}), antimony (Sb(III)) or cobalt (Co(II) ion as counter-cation or incorporated in the HPA structure modifies the redox properties of the HPA, with development of a more favourable distribution of both reduced Mo(V) and oxidized Mo(VI) sites [1,7–10].

In this study, we have used the ammonium salt of 12-molybdophosphoric acid ($(NH_4)_3PMo_{12}O_{40}$) that is micro and mesoporous with a large surface area and which exhibits better thermal stability than the parent acid and we have partially replaced the ammonium ions by antimony, bismuth and tin in order to facilitate electron transfer during redox processes. We report here the synthesis and characterization by BET method, ICP measurements, XRD, ^{31}P NMR, UV–Vis, Raman, IR techniques and thermal analysis (TGA and DTA) of ammonium–antimony, ammonium–bismuth and ammonium–tin mixed phosphomolybdates with Keggin structure in the aim to find correlation between redox properties and the nature of counter-cation.

2. Experimental

2.1. Synthesis

$(NH_4)_3PMo_{12}O_{40}$ (noted NH_4PMo_{12}) and the mixed ammonium salts $(NH_4)_xX_yPMo_{12}O_{40}$ where $X^{n+} = Sb^{3+}, Bi^{3+}, Sn^{2+}$ (noted $XPMo_{12}$) were precipitated at pH < 1 as described by Cavani et al. [11]. For each compound a solution (A) was prepared as follows: 25 g of ammonium heptamolybdate (0.02 mol) was dissolved in 100 mL of water by heating and 1.15 mL of phosphoric acid (85%, 0.01mol) were added. The solution becomes pale yellow. The pH is then equal to 5.5. $(NH_4)_3PMo_{12}O_{40}$ was precipitated by slow addition of concentrated hydrochloric acid (ca. 24 mL, 37%) to a solution A (final pH 0.6). The yellow compound was filtered off and dried overnight at 50 °C. For the preparation of the mixed ammonium salts ($XPMo_{12}$), the solution A was added with 0.01 mol of XCl_3 (Sb or Bi) or XCl_2 (Sn) previously dissolved in the minimum amount of concentrated hydrochloric acid. $XPMo_{12}$ salt was precipitated by slow addition of concentrated hydrochloric acid until pH 0.6 (ca. 25 mL). The precipitate was filtered off and

---

* Corresponding author. Tel./fax: +213 21247311.
E-mail address: c_rabia@yahoo.fr (C. Rabia).

0020-1693/$ - see front matter Published by Elsevier B.V.
doi:10.1016/j.ica.2009.04.049

dried overnight at 50 °C. $BiPMo_{12}$ and $(NH_4)_3PMo_{12}O_{40}$ are yellow but $SnPMo_{12}$ and $SbPMo_{12}$ are dark green.

2.2. Characterization

Inductively coupled plasma spectrometry (ICP) measurements were carried out using a Perkin–Elmer, Optima 2000 D.VS Spectrometer.

BET surface area measurements were performed at liquid nitrogen temperature using a Micrometrics Accusorb 2100E apparatus. Prior to each adsorption–desorption measurement, the samples were degassed at $T = 150\,°C$ for 24 h. The specific surface areas were determined using the linear part of the BET equation.

Infrared spectra were recorded on a Bruker IFS 66 FTIR spectrometer with samples prepared as KBr disks on the 400–4000 cm^{-1} range. Laser Raman spectroscopy data were obtained with a Kaiser Optical Systems Holollab 5000R model, equipped with near-IR laser diode ($\lambda_{exc} = 785$ nm) and CCD detector. The laser power was adjusted to 10 mW at the sample position to prevent local heating effects.

^{31}P MAS NMR spectra were measured at room temperature on a Bruker Avance 400 spectrometer. 85% H_3PO_4 was used as an external reference.

UV–Visible diffuse reflectance spectra were recorded in the 200–800 nm regions on a Varian Cary 5E spectrometer equipped with a polytetrafluoroethylene (PTFE) integration sphere. PTFE was used as a reference.

X-ray diffraction powder patterns were obtained on a D8 Advance Bruker AXS diffractometer using Cu Kα radiation and VANTEK fast detector in HTK16 ANTON PAAR room.

Thermogravimetric and differential thermal data were collected on a SDT-2960 thermal analyzer. The thermogravimetry and differential thermal analysis experiments were performed under air flux, using 25–70 mg samples and a heating rate of 10 °C/min.

3. Results and discussion

1 – The chemical composition determined by ICP and surface area of the heteropolycompounds studied in the present study are shown in Table 1. The results of chemical analysis of salts were adjusted considering 12 atoms of molybdenum per Keggin unit according to the nature of HPA and were found in good agreement with desired stoichiometries for phosphorous and molybdenum for $BiPMo_{12}$ and $(NH_4)_3PMo_{12}O_{40}$ and only for molybdenum for both $SbPMo_{12}$ and $SnPMo_{12}O_{40}$. In these latter's, the amount of phosphorous was found in excess compared to the desired value. This has been attributed to the existence of species containing phosphorous other than HPA, as it was shown in the ^{31}P MAS NMR analysis. The ICP analysis of Bi, Sb or Sn element led to stoichiometries coefficient given in Table 1. It is noted that the amount of bismuth contained in the salt is very low, compared with those of tin and antimony. This could be due to hydrolysis phenomena where the bismuth ions could be sensible.

The surface areas of mixed salts are significantly lower than that of NH_4PMo_{12} (222 m^2/g) and nearly independent of both nature and amount of the substituting cation (ca. 100 m^2/g). The measured surface area of NH_4PMo_{12} is in agreement with literature data [12].

2 – The FTIR spectra of $(NH_4)_3PMo_{12}O_{40}$ and of $XPMo_{12}$, X = Bi, Sb or Sn (Fig. 1), in the low wavenumber region (1100–500 cm^{-1}), are very similar and the characteristic bands of the Keggin structure were observed. According to Rocchiccioli-Deltcheff et al. [13], the bands at 1063, 961, 863, 786 and 561 cm^{-1} correspond to $\nu_{as}(P–O_a)$, $_{as}$ $(Mo–O_d)$, ν_{as} $(Mo–O_b–Mo)$, ν_{as} $(Mo–O_c–Mo)$ and δ (P–O) vibrations respectively. In Keggin-type unit, O_a refers to O atom common to PO_4 tetrahedron and a trimetallic group; O_b to O atom connecting two trimetallic groups, O_c to O atom connecting two MoO_6 octahedral inside a trimetallic group and O_d to the terminal O atom. This structure has Td symmetry and corresponds to α isomer. In addition, the vibration band attributed to ammonium ions was observed at 1403–1407 cm^{-1}. The comparison of the IR frequency of vibration bands of $XPMo_{12}$ salts (Fig. 1) with those of NH_4PMo_{12} did not reveal significant difference within the range 1500–500 cm^{-1}. This suggests that primary structure remains intact and that the ammonium ions are partially replaced in $XPMo_{12}$ salts by the X ions.

3 – The Raman spectra of different salts are shown in Fig. 2. The spectrum of NH_4PMo_{12} in the low wavenumber region (1000–240cm^{-1}) exhibits the characteristic bands of the Keggin unit. According to literature data [14], the bands at 988, 876, 608 and 240 cm^{-1} correspond to $\upsilon_s(Mo = O_d)$, ν_{as} $(M–O_b–Mo)$, $\nu_s(Mo–O_c–M)$ and $\nu_s(Mo–O_a)$ metal-oxygen vibrations respectively. The shoulder at 971 cm^{-1} is attributed to $\upsilon_{as}(Mo = O_d)$. The P–O vibration of PO_4 tetrahedron is Raman-inactive. The observed vibration bands at 988 and 240 cm^{-1} are the more intense. The Raman spectrum of $BiPMo_{12}$ is similar to that of NH_4PMo_{12}. While the partial substitution of ammonium ions by antimony or tin compared to bismuth, has an influence on the metal-oxygen vibration bands. So, in Raman spectra, excepted the $\nu_s(Mo–O_a)$ band which was not modified, that corresponding to $\upsilon_s(Mo = O_d)$ decreased in intensity and its frequency is passed from 988 to 979 cm^{-1}. On the other hand, the shoulder assigned to $\upsilon_{as}(Mo = O_d)$ vibration

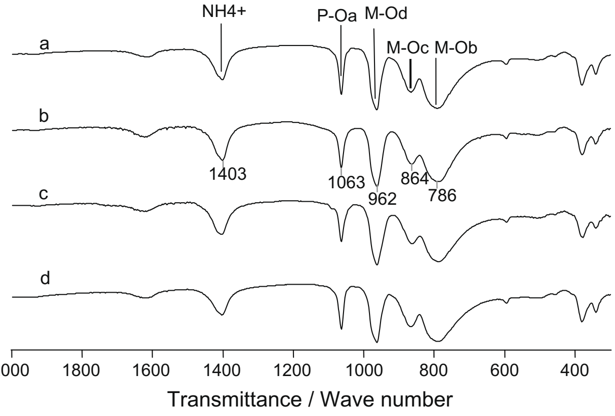

Fig. 1. FTIR spectra of NH_4PMo_{12}, $BiPMo_{12}$, $SbPMo_{12}$ and $SnPMo_{12}$.

Table 1
Chemical composition from ICP and surface area of heteropolycompounds.

Formula	Chemical composition (wt%)			Stoichiometries coefficient			Surface area (m^2/g)
	P	Mo	X	P	Mo	X	
$(NH_4)_3PMo_{12}O_{40}$	1.71	58.42		1.05	12		222
$(NH_4)_{2.988}Bi_{0.004}PMo_{12}O_{40}$	1.68	57.86	60 ppm	1.04	12	0.004	101
$(NH_4)_{0.5}Sn_{1.25}PMo_{12}O_{40}$	1.75	38.94	4.41	1.30	12	0.75	96
$(NH_4)_{0.75}Sb_{0.75}PMo_{12}O_{40}$	2.07	33.32	4.32	2.20	12	1.25	100

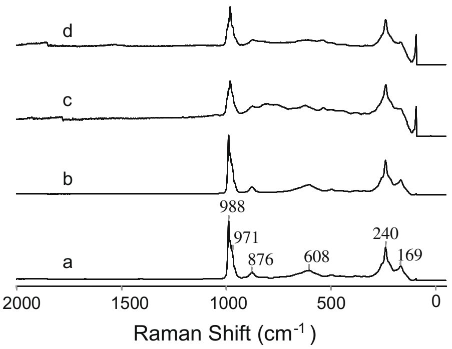

Fig. 2. Raman spectra of NH_4PMo_{12} (a), $BiPMo_{12}$ (b), $SbPMo_{12}$ (c) and $SnPMo_{12}$ (d).

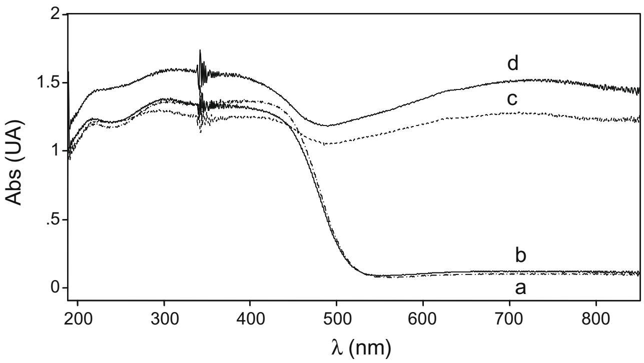

Fig. 4. UV–Visible spectra of NH_4PMo_{12} (a), $BiPMo_{12}$ (b), $SbPMo_{12}$ (c) and $SnPMo_{12}$ (d).

and the bands attributed to ν_{as}(M–O$_b$–Mo) and ν_s(Mo–O$_c$–M) are not clearly visible on spectra in particular in presence of $SnPMo_{12}$. These perturbations were probably caused by the partially reduced state of heteropolyanion, confirmed by the characteristic blue colour of reduced HPA of Keggin-type [15]. Compared to IR spectroscopy, the Raman spectroscopy seems to be sensible to the reduction of molybdenum (VI) induced by antimony and tin.

4 – ^{31}P MAS NMR technique is very sensitive to local chemical environment and surrounding symmetry of phosphor. In ^{31}P NMR analysis, the whole NH_4PMo_{12} and $BiPMo_{12}$ samples gave only one peak, at -4.4 ppm. (Fig. 3) The chemical shift of ^{31}P has been found at -4.4 ppm for $H_3PMo_{12}O_{40}$, a value close to those observed for our samples. However, for $SnPMo_{12}$ and $SbPMo_{12}$ samples, their ^{31}P NMR spectrum could be decomposed in three peaks, one at -4.4 ppm, as major peak, and the two others, as minor peaks, at -0.8 and -7.0 ppm for $SnPMo_{12}$ and at -2.0 and -6.0 ppm for $SbPMo_{12}$. These latter's disappear after pre-treatment at 400 °C under nitrogen. This can indicate that the amount of impurities, if it is present, it must be low. Theses impurities explain the excess of phosphorous observed par ICP analysis for these two salts.

5 – UV–Visible diffuse reflectance seems to be a very appropriate technique to distinguish the electronic properties of the Mo ions. In the UV–Vis spectra of salts (Fig. 4), a large band in the domain of wavelengths 200–400 nm was observed with multiplicity for all samples. It is constituted of several components (200–250, 270–350, and 400–450 nm ranges) having different energies associated to ligand–metal charge transfers (LMCT) from oxygen to Mo(VI) in the Keggin anion. This result has been also observed by other authors that suggested that the presence of more than one band in the spectrum of Keggin-type compound is attributed to different oxygen ions and to inter-anion charge transfer transitions [8,16–18]. On the other hand, these energies have been also associated to cationic composition of the Keggin secondary framework as the crystallinity of the compound and oxidation potential of the oxometal. In addition to this broad absorption band, another large charge transfers band was observed above 700 nm for both $SnPMo_{12}$ and $SbPMo_{12}$ samples, that may be attributed to the d–d transition band of d^1 Mo(V) species in octahedral coordination [10,19–21]. This result suggested a partial reduction of Mo(VI) to Mo(V) in both $SnPMo_{12}$ and $SbPMo_{12}$ salts corresponding to the electron exchange occurring between Sb(III) or Sn(II) and Mo(VI) as follows:

$$Sn^{II} + 2Mo^{VI} \leftrightarrow Sn^{IV} + 2Mo^{V}, \quad Sb^{III} + 2Mo^{VI} \leftrightarrow Sb^{V} + 2Mo^{V}$$

The increase of the intensity of this band corresponds to the increase of the concentration of Mo(V) ions in the polyoxometalate [8]. Thus, these results suggest that the reduction of this last one is more important in the presence of tin than of antimony.

The brown colour of both $SnPMo_{12}$ and $SbPMo_{12}$ salts disappears after a pre-treatment at 400 °C under molecular oxygen, during 4 h and becomes yellow, colour of the $(NH_4)_3PMo_{12}O_{40}$ salt. On the other hand, the UV–Vis spectrum of pre-treated $SnPMo_{12}$ salt (Fig. 5) shows that the intensity of adsorption band at 700 nm has decrease, indicating that the Mo(V) ions were oxidized to Mo(VI) ions. Similar results were obtained with $SbPMo_{12}$ (figure not represented here). These results, in agreement with those of the Raman spectroscopy, confirm that the introduction of tin and antimony led to partially reduced phosphomolybdate.

6 – The thermal stability of the salts was investigated by means of thermogravimetric (TG) and differential thermal analysis (DTA)

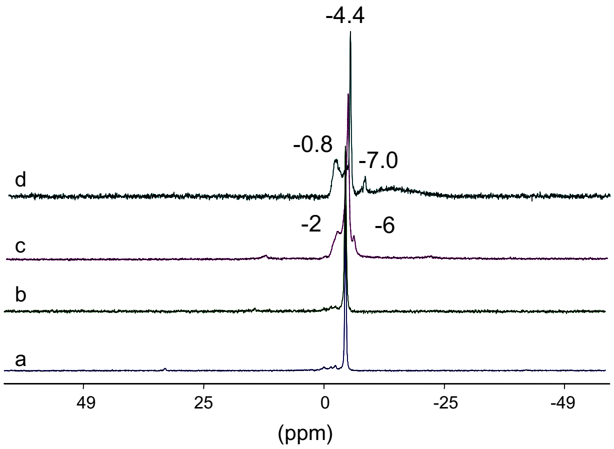

Fig. 3. ^{31}P MAS NMR spectra of NH_4PMo_{12} (a), $BiPMo_{12}$ (b), $SbPMo_{12}$ (c) and $SnPMo_{12}$ (d).

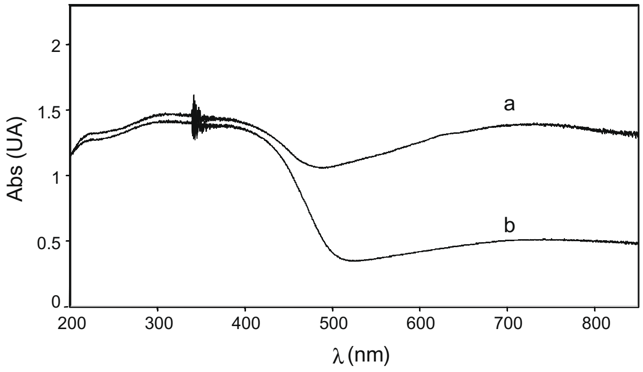

Fig. 5. UV–Visible spectrum of $SnPMo_{12}$, (a): before thermal treatment, (b): after thermal treatment (400 °C/4h/O_2).

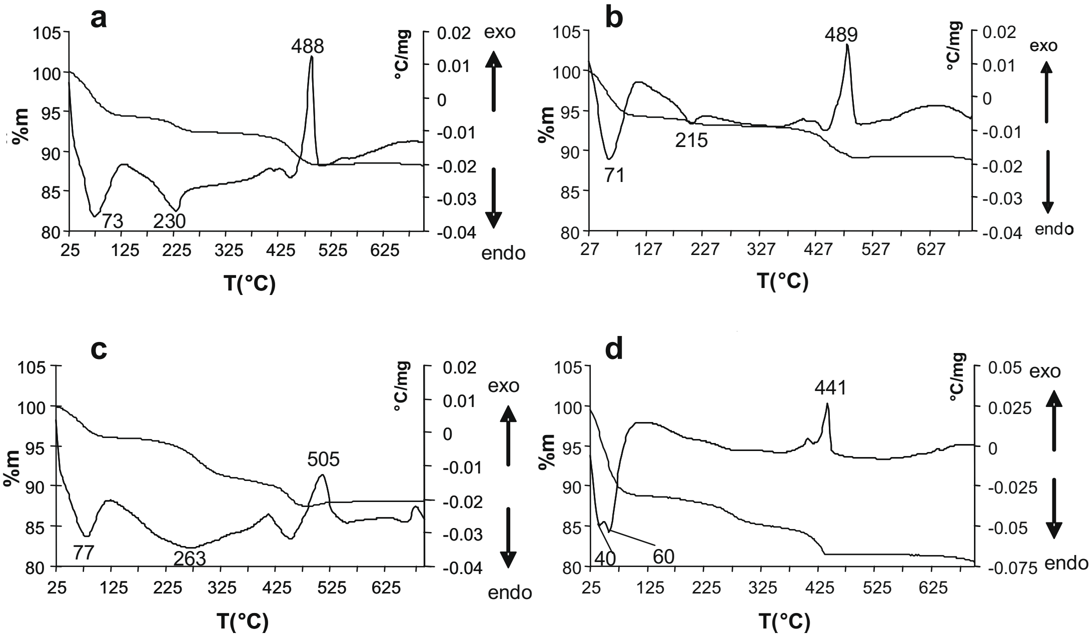

Fig. 6. TG–DTA diagrams of NH_4PMo_{12} (a), $BiPMo_{12}$ (b), $SbPMo_{12}$ (c) and $SnPMo_{12}$ (d).

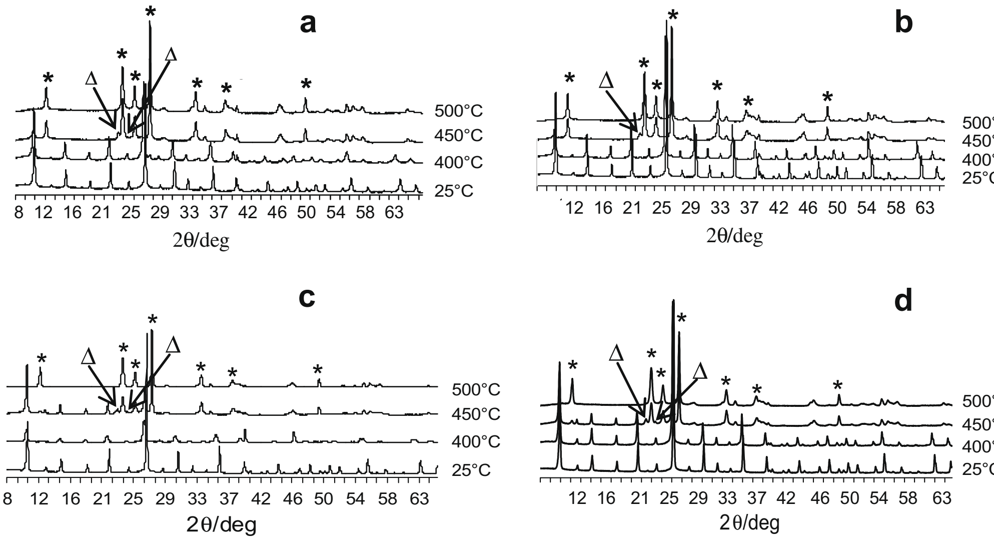

Fig. 7. XRD patterns of NH_4PMo_{12} (a), $BiPMo_{12}$ (b), $SbPMo_{12}$ (c) and $SnPMo_{12}$ (d).

(Fig. 6). The TG curve of NH_4PMo_{12} salt (Fig. 6a) shows that there are three steps of weight loss. Before 200 °C, weight loss (5.7 wt%) attributed to crystallisation water desorption and between 200–500 °C weight loss (5.5 wt%) which was conducted in two steps, assigned to ammonium ions departure. In the DTA curve (Fig. 6a), two endothermic peaks were observed at 73 and 228 °C, associated to the different mass losses observed in TG. A wide exothermal signal assigned to NH_4PMo_{12} decomposition with maximum at 488 °C and another small exothermic peak resulting from the exothermic crystallization of both P_2O_5 and MoO_3 oxides at 559 °C were observed.

The TG curves of mixed salts (Fig. 6b–d) are similar to that of NH_4PMo_{12} salt with weight-losses divided into three major events. The total mass loss is of 11.73, 10.68, 12.52 and 18.47 wt% for NH_4PMo_{12}, $BiPMo_{12}$, $SbPMo_{12}$ and $SnPMo_{12}$ respectively. It is to note that the amount of weight released from both $SbPMo_{12}$ and $SnPMo_{12}$ is higher than that from both NH_4PMo_{12} and BiPMo12. This is probably due to high hydration degree of Sb and Sn cations whose the stoichiometric coefficient is the highest (0.74 and 0.94, respectively).

The area of endothermic peaks assigned to the losses of mass corresponding to the water and to the ammonium ions, in the case of substituted salts, seems to be related with both number and nature of cations incorporated as observed in TG curves. Thus, it is more important in the case of $SnPMo_{12}$ and $SbPMo_{12}$. The complete decomposition of substituted salts corresponds to the broad exothermic effect with maxima at 481, 510 and 441 °C for $BiPMo_{12}$, $SbPMo_{12}$ and $SnPMo_{12}$ respectively.

According to the TG–DTA studies, the decomposition of $BiPMo_{12}$ and that of $SbPMo_{12}$ take place at a temperature similar to that of

NH_4PMo_{12} (488–505 °C). However, for the $SnPMo_{12}$ sample, the thermal stability is lower, probably due to strong reducing character of tin ions as shown in UV–Visible.

7 – Fig. 7 shows that the XR diffractograms of $XPMo_{12}$ are similar to that of NH_4PMo_{12} whose the structure is cubic (JCPDS 09-0412). This is suggested that the X ions have occupied the counter-ion position in the polyoxometalate.

Besides, the examined thermal stability by TG–DTA, the structural stability of salts has been studied as a function of the temperature of thermal treatment. Fig. 7 shows X-ray diffractograms of salts at 25 °C and after treatment under air at following temperatures 400, 450 and 500 °C. It was found a similar evolution of XRD profiles for all compounds independent of their starting composition.

The XRD spectra's of all salts after treatment at 400 °C, are similar to those observed at 25 °C. This indicates that all samples maintain the cubic phase when most of its ammonium cations were eliminated as observed in TG analysis. This phenomenon agrees with that observed by Sultan et al. [5]. After treatment at 450 °C, for all salts, the XRD analysis shows the formation of molybdenum trioxide in the monoclinic form (β MoO_3) and in the orthorhombic form (α MoO_3). These two species were already observed by Rocchiccioli-Deltcheff et al. [22] in the case of the decomposition of 12-molybdophosphoric acid. After treatment at 500 °C only orthorhombic α MoO_3 was detected showing that β MoO_3 was transformed into α MoO_3.

The decomposition temperature of salts to oxides obtained by the XRD analysis is weaker than that observed in DTA (450 °C against 489, 481 and 510 °C).

4. Conclusion

The obtained results in this study showed that the substituted salts have the Keggin structure and the cubic structure of pure ammonium salt NH_4PMo_{12}. The presence of the charge transfer between the tin (or antimony) counter-cation and molybdenum (VI) in the Keggin unit has been shown by UV–Visible analysis. Thus, the introduction of tin and antimony can lead to partially reduced phosphomolybdates with a lower thermal stability for tin based salt.

References

[1] M. Langpape, J.M.M. Millet, Appl. Catal. A: Gen. 200 (2000) 89.
[2] W. Ueda, Y. Suzuki, Chem. Lett. (1995) 541.
[3] W. Ueda, Y. Suzuki, W. Lee, S. Imaoka, Stud. Surf. Sci. Catal. 101 (1996) 1065.
[4] F. Cavani, R. Mezzogori, A. Pigamo, F. Trifiro, C.R. Acad. Chim. 3 (2000) 523.
[5] M. Sultan, S. Paul, M. Fournier, D. Vanhove, Appl. Catal. A: Gen. 259 (2004).
[6] W. Li, K. Oshihara, W. Ueda, Appl. Catal A: Gen 182 (1999) 357.
[7] R. Bayer, M. Marchal, F.X. Liu, A. Tézé, G. Hervé, J. Mol. Catal. 110 (1996) 65.
[8] F. Cavani, R. Mezzogori, A. Pigamo, F. Trifiro, Chem. Eng. J. 82 (2001) 33.
[9] Q. Huynh, J.M.M. Millet, J. Phys. Chem. Sol. 66 (2005) 887.
[10] T. Mazari, C. Roch. Marchal, S. Hocine, N. Salhi, C. Rabia, J. Nat. Gas Chem., in press.
[11] F. Cavani, R. Mezzogori, A. Pigamo, F. Trifiro, Surf. Chem. Catal. 3 (2000) 523.
[12] S. Albonetti, F. Cavani, F. Trifiro, M. Gazzano, M. Koutyrev, F.C. Aissi, A. Aboukais, M. Guelton, J. Catal. 146 (1994) 491.
[13] C. Rocchiccioli-Deltcheff, M. Fournier, R. Frank, R. Thouvenot, Inorg. Chem. 22 (1983) 207.
[14] C. Rocchiccioli-Deltcheff, R. Thouvenot, R. Frank, Spectrochim. Acta 32A (1976) 587.
[15] C. Marchal-Roch, C. Julien, J.F. Moisan, N. Leclerc-Laronze, F.X. Liu, G. Hervé, App. Catal. A 278 (2004).
[16] C. Rocchiccioli-Deltcheff, A. Aoussi, M.M. Bettahar, S. Launay, M. Fournier, J. Catal. 164 (1996) 16.
[17] Ch. Srilakshmi, N. Lingaiah, I. Suryanarayana, P.S. Sai Prasad, K. Ramesh, B.G. Anderson, J.W. Niemantsverdriet, Appl. Catal. A: Gen. 296 (2005) 54.
[18] M. Fournier, C. Louis, M. Che, P. Chaquin, D. Masure, J. Catal. 119 (1989) 400.
[19] Carmen I. Cabelloa, Irma L. Botto, Horacio J. Thomas, App. Catal. A 197 (2000).
[20] C. Thomazeau, V.Martin.P. Afanasiev, Appl. Catal. A: Gen. 199 (2000) 61.
[21] F. Cavani, R. Mezzogori, A. Pigamo, F. Trifiro, E. Etienne, Catal. Today 71 (2001) 97.
[22] C. Rocchiccioli-Deltcheff, A. Aouissi, S. Launay, M. Fournier, J. Mol. Catal. A Chem. 114 (1996) 33l.